Probabilistic dynamic amplification of Australian B-Double trucks

Shiyi Mei
PhD Candidate, Department of Civil Engineering, Monash University,Melbourne,Australia

Colin Caprani
Associate Professor, Department of Civil Engineering, Monash University,Melbourne,Australia

Daniel Cantero
Associate Professor, Department of Structural Engineering, Norwegian University of Science & Technology NTNU,Trondheim,Norway

ABSTRACT: Traffic loading is one of the most common and important live loads to which bridges are subjected. In particular, the dynamic effect caused by running vehicles plays an important role in determining the structural safety of bridges subjected to traffic loading. The Dynamic Amplification Factor (DAF) is widely used to determine dynamic stresses in bridges. Many researchers have modeled the actions of rigid vehicles or semi-trailers by Vehicle-Bridge-Interaction (VBI) simulations. However, far less research has focused on the probabilistic analysis of typical 9-axle B-Double heavy vehicles which feature a tractor and two trailers. For these vehicles, this work develops the relationship between the DAF, static bending moment at mid-span bridge, and Gross Vehicle Mass (GVM) through Monte Carlo (MC) simulation with a set of observed B-Double parametric data. The outcome of this study provides a quick and simple way to predict the interaction between 9-axle B-Double vehicles and common types of simply supported bridges in Australia under different classes of road profile conditions.

1. INTRODUCTION

The serviceability and safety of highway bridges is significantly affected by traffic loading which is determined by running vehicles. High Productivity Vehicles (HPFV) with large gross vehicle weight (GVM) are very common and lead to higher load effects compared to rigid vehicles (Caprani, 2005). B-Double vehicles are one of the most common multi-body heavy vehicles in Australia (The Drake Group, 2018). Therefore there is a need to study how B-Doubles affect the common bridge structures in Australia. Due to the traffic freight demand and its configuration, the gross mass of the B-Double is relatively high compared to other semi-trailers and can reach 69 tonnes (Regulator, 2016). In fact, traversing vehicles not only induce static load but also additional dynamic load onto the bridge. To evaluate these load effects on the bridge, the Dynamic Amplification Factor (DAF) can be considered as am important indicator (OBrien et al., 2021b). The Vehicle Bridge Interaction (VBI) technique has an significant advantage on investigating the bridge response induced by vehicles compared to field study which is costly and time consuming. This method also makes it convenient and efficient to implement statistical analysis on different types of vehicles and bridges. The dynamic response of bridges induced by rigid vehicles, semi-trailers with five or six axles, and 7-axle B-Double trucks have been investigated by many researchers in the past decade (Zhu and Law, 2002; González et al., 2008;

Cantero et al., 2009; Meyer et al., 2021). However there is less research on the 9-axle B-Double which has more axles configuration compared to these vehicle types.

For the assessment of existing bridges, in particular, it is critical to avoid undue conservatism in the live load model to which the bridge is assessed. Currently there is little information on the DAFs appropriate for assessment, beyond some field trials and estimates (Melhem et al., 2020). As shown in Caprani (2013) and OBrien et al. (2021a), it is well known that the DAFs appropriate for extreme static loading events are not the same as those that are measured or modelled under regular traffic. Consequently, there is a need to quantify the probabilistic nature of DAFs for the B-double truck to improve bridge assessments in Australia. This work provides a comprehensive VBI model of these trucks and couples it with extensive simulations to examine the extreme total load effect, and the appropriate DAF for lifetime extremes.

2. Study Methodology

Six months of Weigh-In-Motion (WIM) data were recorded at the West Gate Bridge in Melbourne in 2016. This data was processed to identify the B-double trucks, using standard WIM cleaning and vehicle categorization techniques (e.g. Melhem et al. (2020); OBrien et al. (2021a)). From this, 18 000 9-axle B-double trucks were identified: in particular the axle masses and spacings are found. This extensive set of measurements is taken to reliably represent the typical loading profile of these vehicles in the Australian road network.

Prestressed-concrete Super-T girders are a common form of bridge structure in Australia, economic for most spans around 15 to 35 m or so. Three typical super T bridge types (18 m, 28 m and 38 m) are considered for this work. These spans cover the range, and so inference on intermediate spans can be estimated.

Generally speaking, road condition on Australia's main highway and freight routes are quite good. As such, Classes A, B and C road profiles are used for this study.

A Monte Carlo Simulation strategy is used, based on the above settings, to provide an estimate of the distribution of 9-axle B-double DAFs. In total, 1×10^5 loading events are simulated to obtain the results for this work.

Section 3 presents an introduction to the models of common 9-axle B-Double truck, bridges and the coupled VBI algorithm. The investigation based on the MC simulation supported by WIM data is shown in Section 4.

3. Vehicle Bridge Interaction Model

3.1. *Vehicle Model*

The 9-axle B-Double vehicle is a common High productive freight vehicle (HPFV) in Australia which consists of a tractor and two semi-trailers both with three axles shown in Figure 1. There are two articulations (fifth wheels) connecting the tractor, first and second trailers. The tractor and trailers are simulated as lumped mass rigid bodies and are connected with concentrated axle mass particles by suspension system, where tyres support the axles and contacts with the road surface. The suspension and tyre systems are idealized as dashpot-spring configuration shown in Figure 2.

The equations of motion of the 9-axle B-Double can be expressed in matrix form as:

$$\left[\mathbf{M_v}\right]\left\{\ddot{\mathbf{q}}\right\} + \left[\mathbf{C_v}\right]\left\{\dot{\mathbf{q}}\right\} + \left[\mathbf{K_v}\right]\left\{\mathbf{q}\right\} = \left\{\mathbf{F_v}\right\} \quad (1)$$

The DOFs are defined by the generalized coordinates as:

$$\mathbf{q} = \begin{bmatrix} q_1 & q_2 & q_4 & q_6 & q_7 & q_8 & q_9 & \cdots & q_{15} \end{bmatrix}^T \quad (2)$$

where q_1, q_2, q_4 and q_6 represent the vertical tractor displacement, tractor pitch rotation, first trailer pitch rotation and second trailer pitch rotation respectively. The vertical axles displacement are denote as q_7 to q_{15}. The force vector is given by:

$$\mathbf{F}_v = \begin{bmatrix} \mathbf{0}_{(4\times 1)} & f_1 & f_2 \cdots & f_9 \end{bmatrix}^T \quad (3)$$

where f_i is the contact force caused by the road roughness r_i and bridge displacement y_{bi} at the i-th wheel of vehicle, which is defined by:

$$f_i = k_t^i\left(r_i + y_{bi}\right) + c_t^i\left(\dot{r}_i + \dot{y}_{bi}\right) \quad (4)$$

where k_t^i and c_t^i are the i-th tyre stiffness and damping.

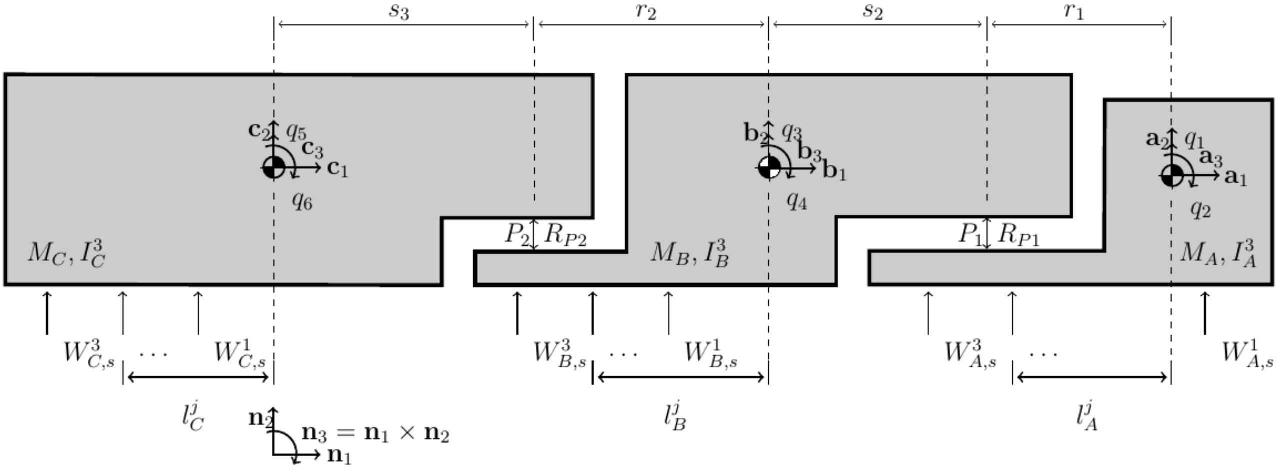

Figure 1: Dynamic truck model of a B-double truck with arbitrary axles.

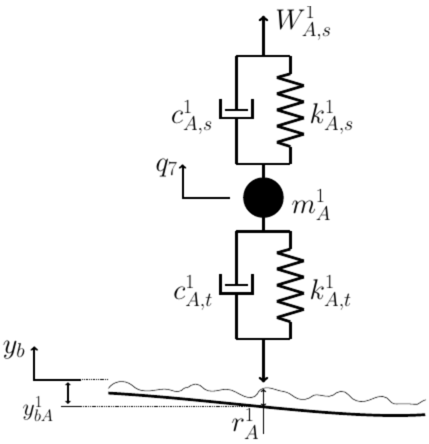

Figure 2: Dynamic model of an individual axle in the B-double model, Figure 1.

3.2. Bridge Model

The simply supported Euler-Bernoulli beam which has been widely applied for bridge simulation is considered in this study. There are mainly two approaches to the bridge model: modal superposition method (MSM) and finite element (FE) method. The first method provides the analytical solution of the Euler-Bernoulli beam theory and usually the first few mode shapes are considered. However bridge model may be difficult to derive by MSM due to the complexity of characteristic equations determined by the boundary condition. The FE method provides a high precision approximation solution to the bridge which easily accommodates bridge structures with complex boundary conditions. It provides perfect results matching the MSM when sufficient numbers of elements are considered. It should be noticed that MSM typically has a lower matrix dimension than FE for the bridge. Nevertheless, bridge models derived from both methods can be expressed in the matrix form by:

$$\left[\mathbf{M_b}\right]\left\{\ddot{\mathbf{q}}_b\right\}+\left[\mathbf{C_b}\right]\left\{\dot{\mathbf{q}}_b\right\}+\left[\mathbf{K_b}\right]\left\{\mathbf{q}_b\right\}=\left\{\mathbf{F_b}\right\} \tag{5}$$

where $\mathbf{F_b}$ contains the static wheel loads and contatcing interaction forces, $\mathbf{q}_b$ is vector of modal coordinates for MSM models, vector of nodal displacements for FE bridge.

3.3. Coupled Vehicle Bridge Interaction

The equations of motion of the vehicle and the bridge are coupled to form global matrices which meet the compatibility condition between the vehicle and the bridge. The coupled VBI equations are given by:

$$\begin{bmatrix}\mathbf{M}_v & 0\\ 0 & \mathbf{M}_b\end{bmatrix}\begin{Bmatrix}\ddot{\mathbf{q}}\\ \ddot{\mathbf{q}}_b\end{Bmatrix}+\begin{bmatrix}\mathbf{C}_v & \mathbf{C}_{vb}\\ \mathbf{C}_{bv} & \mathbf{C}_b+\mathbf{C}_{bb}\end{bmatrix}\begin{Bmatrix}\dot{\mathbf{q}}\\ \dot{\mathbf{q}}_b\end{Bmatrix}+\begin{bmatrix}\mathbf{K}_v & \mathbf{K}_{vb}\\ \mathbf{K}_{bv} & \mathbf{K}_b+\mathbf{K}_{bb}\end{bmatrix}\begin{Bmatrix}\mathbf{q}\\ \mathbf{q}_b\end{Bmatrix}=\begin{Bmatrix}\mathbf{0}_{(5\times1)}\\ \mathbf{F}_v\\ \left[\mathbf{N}\right]\left\{\mathbf{F_b}\right\}\end{Bmatrix} \tag{6}$$

where the shape matrix $\mathbf{N}$ describes the location of the wheels' dynamic forces and it varies with time.

The submatrices $\mathbf{K}_{vb}$, $\mathbf{K}_{bv}$, $\mathbf{C}_{vb}$ and $\mathbf{C}_{bv}$ are related to shape matrix.

4. Simulation Results

The VBI developed in the previous section is applied to simulate the interaction scenarios between the bridge and 9-axle-B-Doubles using the data and settings described earlier. For the present work a fixed velocity of 100 $\mathrm{km\,h^{-1}}$. The results are explained in the following sections.

4.1. *Relation between DAF and GVW*

The influence of gross vehicle mass on DAF are shown in Figures 3 to 5, in which a general decrease in DAF caused by increasing GVW are obtained. Figures 3d, 4d and 5d indicate for all three types of bridges road roughness can increase amplification, especially for lighter vehicles. It can be seen in Figure 4d that for B-Doubles with GVW less than 30000 kg, vehicles with weight around 18000 kg have the lowest amplification for 28 m bridges. This is caused by the bridge's critical load velocity which depends on the vehicle configuration and traversing velocity. Higher levels of DAF could be obtained when critical load velocities matches with the natural frequencies of the bridge, but often these are far beyond normal travelling speeds.

4.2. *Relation between static and total bending moment*

A strong positive linear relationship between static and total bending moment is found, as is expected (OBrien et al., 2021a). Figure 6 shows the correlation coefficients (r) of 0.996, 0.995 and 0.993 for 18 m length span with class A, B and C road conditions respectively. A similar strong linear correlation is obtained from other bridge types and roads. Table 1 shows the slopes (μ), intercepts (c) and residual standard errors (ε) of linear regression between static bending moment and total bending moment for all three types of spans and road roughness. These parameters are useful for probabilistic modelling of total bending moments from static effects of B-double trucks as may be used in a probabilistic bridge assessment, for example.

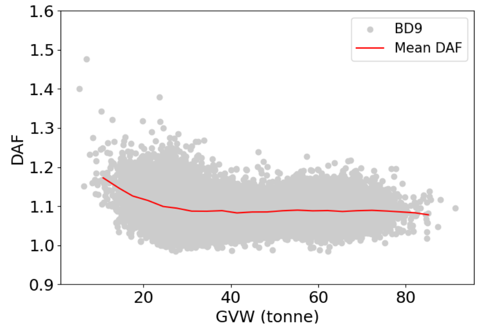

(a)

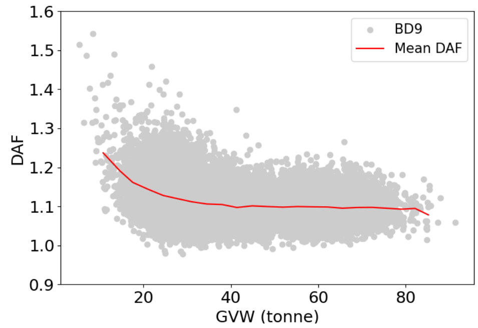

(b)

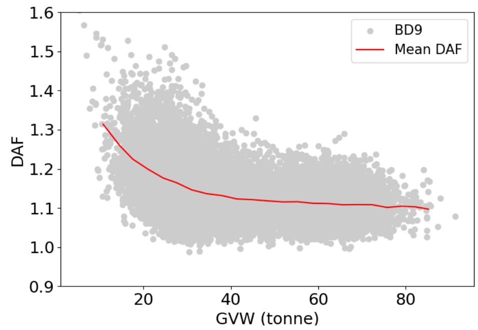

(c)

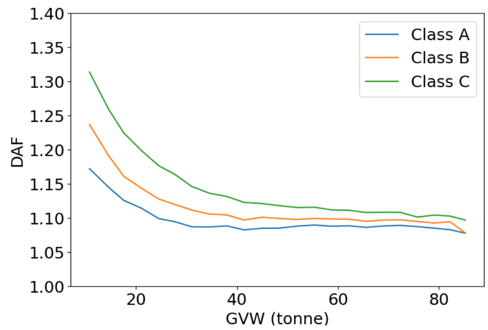

(d)

Figure 3: DAF of 18 m bridge vs GVW of B-Double for: (a) Class A road; (b) Class B road; (c) Class C road; (d) Class A to C.

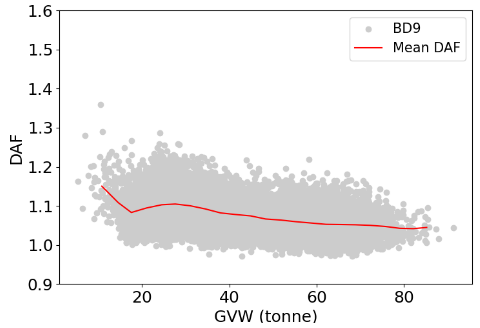

(a)

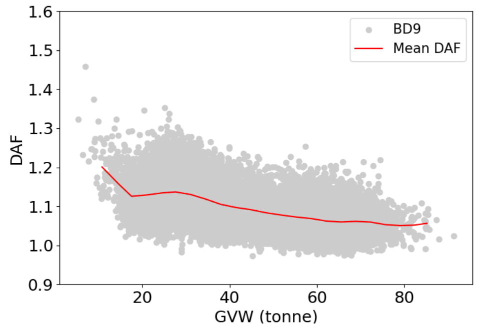

(b)

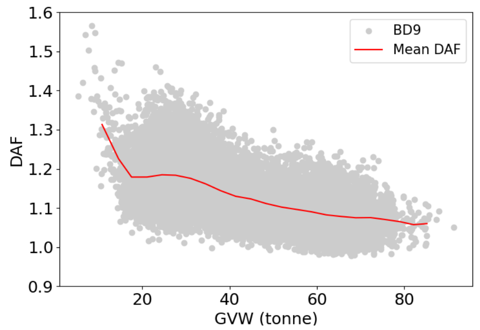

(c)

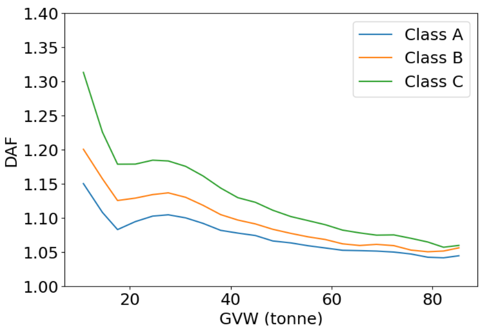

(d)

Figure 4: DAF of 28 m bridge vs GVW of B-Double for: (a) Class A road; (b) Class B road; (c) Class C road; (d) Class A to C.

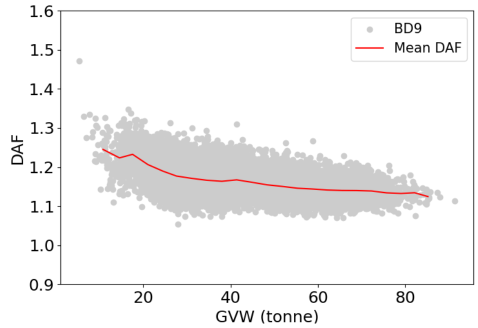

(a)

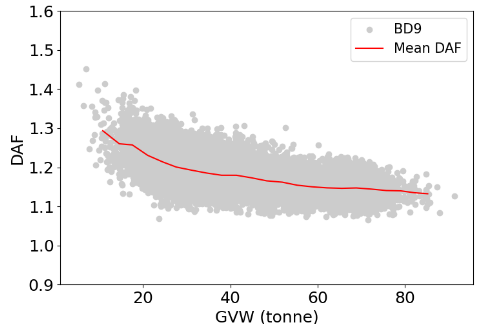

(b)

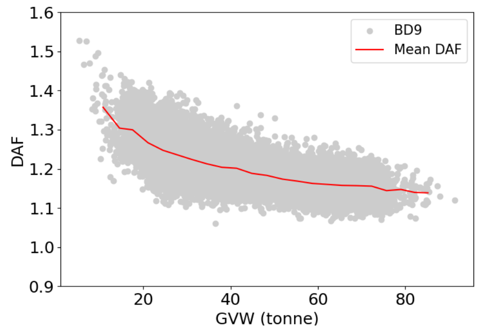

(c)

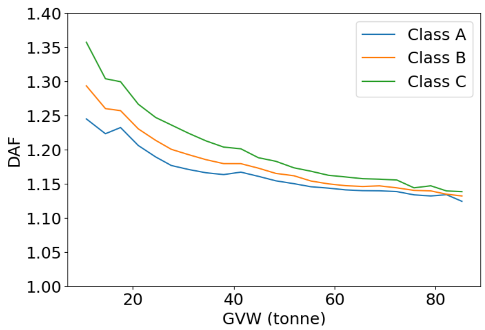

(d)

Figure 5: DAF of 38 m bridge vs GVW of B-Double for: (a) Class A road; (b) Class B road; (c) Class C road; (d) Class A to C.

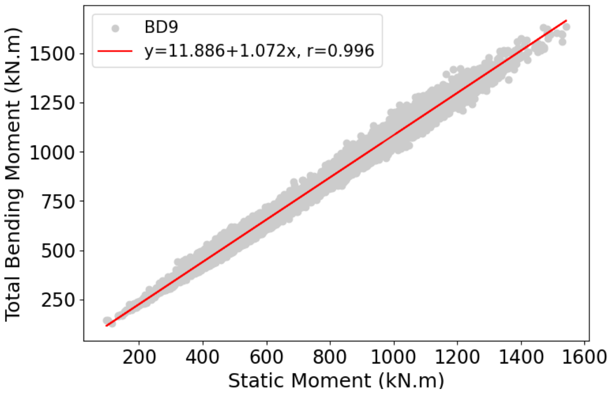

(a)

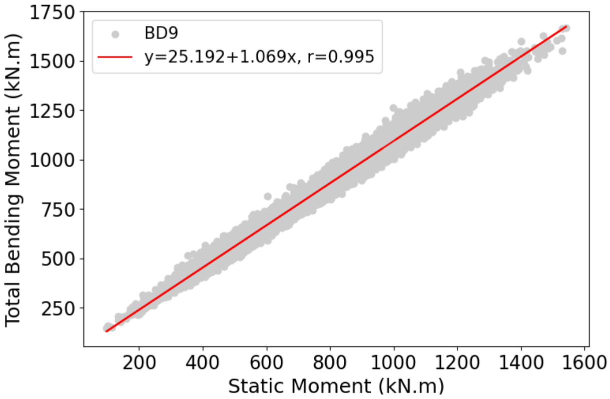

(b)

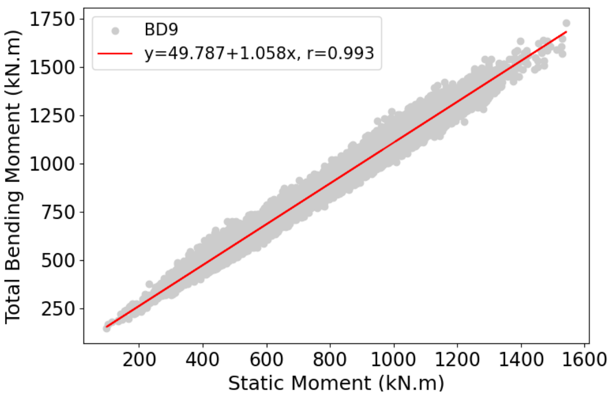

(c)

Figure 6: Correlation between static bending moment and total bending moment of 18 m span length: (a) Class A road; (b) Class B road; (c) Class C road.

Table 1: Slopes, intercepts and residual standard errors of linear regression.

Road Roughness		Span length 18 m	28 m	38 m
Class A	c	11.886	73.696	104.998
	m	1.072	1.025	1.117
	ε	0.192	0.450	0.555
Class B	c	25.192	108.771	148.176
	m	1.069	1.021	1.113
	ε	0.219	0.531	0.625
Class C	c	49.787	156.763	206.763
	m	1.058	1.021	1.110
	ε	0.260	0.644	0.730

4.3. Relation between DAF and static bending moment

Consistent with the literature (e.g. OBrien et al. (2021a)), the maximum static bending moment is found to have a negative relation with amplification which is similar to the results of DAF and GVW in-Section 4.1. Figure 7 shows the scatter plot of DAF and static bending moment for 3 types of bridge lengths (18 m, 28 m and 38 m) when Class A road is considered. Since the static bending moment does not depend on the road profile, the marginal histogram of static bending moment is constant under different road conditions while the distribution of DAF varies. The static bending moment histogram indicates similar distribution shapes for the three bridge types.

Figure 7 shows most of the static bending moments are around 450 $\mathrm{kN\,m^{-2}}$ and 1000 $\mathrm{kN\,m^{-2}}$ for 18 m length, 950 $\mathrm{kN\,m^{-2}}$ and 2400 $\mathrm{kN\,m^{-2}}$ for 28 m length and 1500 $\mathrm{kN\,m^{-2}}$ and 4000 $\mathrm{kN\,m^{-2}}$ for 38 m length. The upper 95 percentile of mean DAF is plotted as dashed line which is parallel above the mean DAF as shown in Figure 7.

To study the characteristic B-Double 9 vehicles, the static moment of the heaviest 95 percent vehicle is chosen and the corresponding upper 95 percentile of DAF is selected to represent the DAF of fully loaded B-Double 9. The results of three bridge and road types are shown in Figure 8 which indicates the 38 m length has the highest level of amplification and 28 m has the lowest, and the worse road condition leads to higher DAF. It can also be seen that for the 18 m length the DAF increase from 1.133 to 1.142 and 1.162 when the class level varies from A to B and C; for 28 m, the values are 1.108, 1.127 and 1.155; and for 38 m, the values are 1.177, 1.193 and 1.212. Compared to lighter vehicles there is less influence of roughness on amplification.

5. Conclusion

This paper presents an effective method to explore the probabilistic dynamic interaction between the common 9-axle B-Double truck and a common bridge type in Australia. Over 18 000 B-Doubles data recorded at the WIM station are utilized to obtain the DAF values. The numerical results suggest that an inverse relationship between DAF and the GVW which consistent with the literature. The heaviest 95 percent vehicle is chosen to represent fully loaded B-Doubles and the upper 95 percentile of DAF corresponding to this GVW is found. This result can be used to assist with probabilistic bridge assessments. The suggested regression parameters to forecast the total dynamic bending moment at mid-span of three common bridge types is also given. The values found are far below the 1.30 typically used for design and assessment in Australia. Such as, these preliminary results obtained from the time-saving and economical approach can help to reduce unnecessary conservatism from bridge assessments.

This study is limited to a single full highway speed, and it should be noted that the vehicle speed plays an important role in the dynamic effect. Therefore, a normal range of vehicle speeds are required in the future studies as a complement to improve its design and assessment purposes.

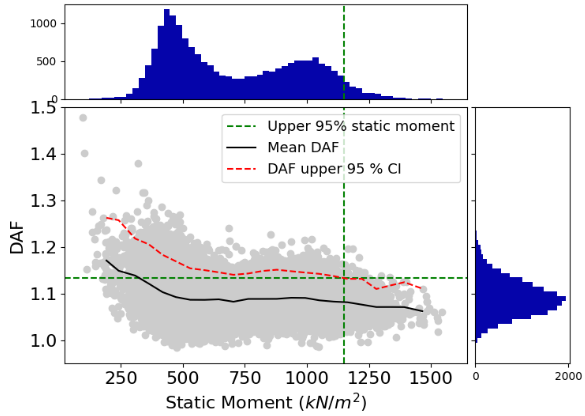

(a)

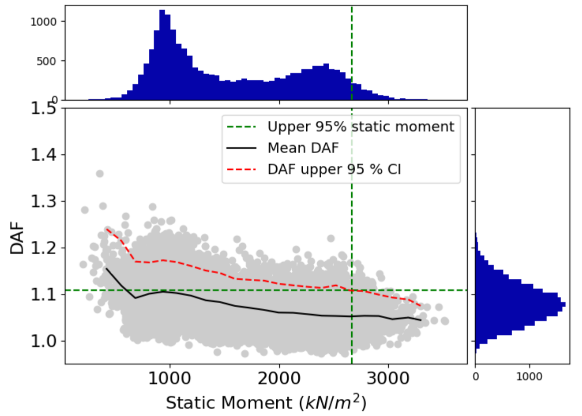

(b)

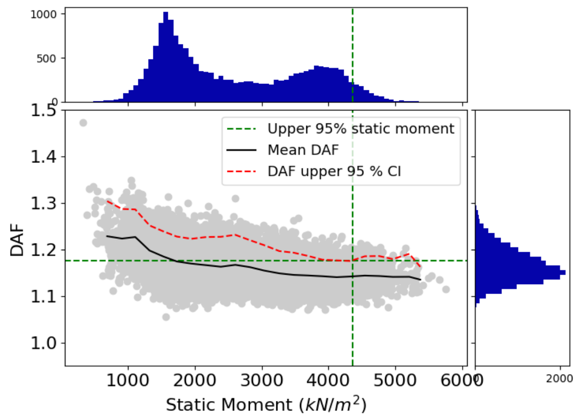

(c)

Figure 7: Scatter plot of DAF and static bending moment with marginal histograms under Class A road condition of: (a) 18 m bridge; (b) 28 m bridge; (c) 38 m bridge.

6. REFERENCES

Cantero, D., González, A., and OBrien, E. J. (2009). "Maximum dynamic stress on bridges traversed by moving loads." *Proceedings of the Institution of Civil Engineers-Bridge Engineering*, Vol. 162, Thomas Telford Ltd, 75–85.

Caprani, C. (2013). "Lifetime highway bridge traffic

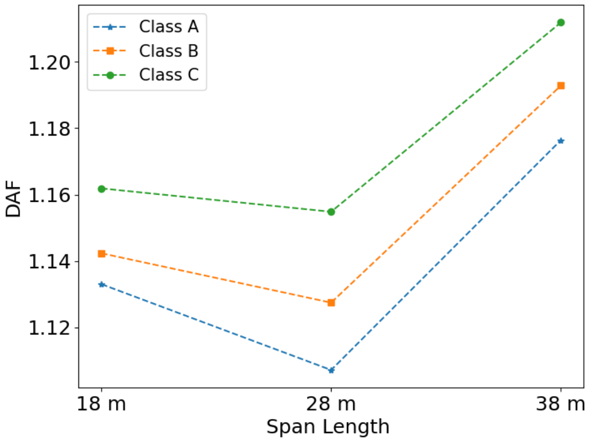

Figure 8: Characteristic DAF of the 95-percentile 9-axle B-Double truck.

load effect from a combination of traffic states allowing for dynamic amplification." *Journal of Bridge Engineering*, 18(9), 901 – 909.

Caprani, C. C. (2005). "Probabilistic analysis of highway bridge traffic loading." Ph.D. thesis, University College Dublin, Dublin, Ireland (October).

González, A., Rattigan, P., OBrien, E. J., and Caprani, C. (2008). "Determination of bridge lifetime dynamic amplification factor using finite element analysis of critical loading scenarios." *Engineering structures*, 30(9), 2330–2337.

Melhem, M., Caprani, C., Stewart, M. G., and Zhang, S. (2020). "Bridge assessment beyond the as 5100 deterministic methodology.

Meyer, M., Cantero, D., and Lenner, R. (2021). "Dynamics of long multi-trailer heavy vehicles crossing short to medium span length bridges." *Engineering Structures*, 247, 113149.

OBrien, E., Nowak, A., and Caprani, C. (2021a). *Bridge traffic loading*. CRC Press, London (October).

OBrien, E., Nowak, A., and Caprani, C. (2021b). *Bridge traffic loading: From research to practice*. CRC Press.

Regulator, N. H. V. (2016). "National class 2 b-double operator's guide.

The Drake Group (2018). "What is a b-double?, <thedrakegroup.com.au/drake-trailers-news/what-is-a-b-double/>.

Zhu, X. and Law, S. (2002). "Dynamic load on continuous multi-lane bridge deck from moving vehicles." *Journal of Sound and Vibration*, 251(4), 697–716.